

## Electrophysiological Characterization of the Ionic Selectivity of Necturus Proximal Tubule

MARY F. ASTERITA

Northwest Center for Medical Education  
Indiana University of Medicine, Gary, Indiana  
and

EMILE L. BOULPAEP

Yale University School of Medicine  
New Haven, Connecticut 06510

### Abstract

The characteristics of transepithelial conductance in the proximal tubules of the kidney of the amphibian, *Necturus maculosus* was assessed by employing electrophysiological techniques.

Changes in luminal cell membrane,  $\Delta V_2$ , peritubular cell membrane,  $\Delta V_1$ , and transepithelial potential,  $\Delta V_3$  were monitored during unilateral salt dilutions in the peritubular capillaries, *p*, or in the lumen, *l*, or bilaterally in both the peritubular capillaries and lumen simultaneously, *pl*. Transference numbers for sodium and chloride were evaluated from the voltage deflection of  $V_3$  induced across the epithelium by these salt dilutions. Actual changes in the electromotive forces induced by salt dilutions across the peritubular membrane,  $\Delta E_1$ , luminal membrane,  $\Delta E_2$ , and paracellular path or extracellular shunt path,  $\Delta E_3$  were estimated by solving a set of simultaneous equations using  $\Delta V_1$  and  $\Delta V_3$  during *p*, *l*, or *pl*, the luminal to peritubular cell membrane resistance ratio, and the specific transepithelial resistance. The results indicate that the proximal tubule exhibits a marked degree of anionic selectivity. Also, the observed transepithelial potential changes closely approximate the actual changes in electromotive force induced across the paracellular pathway and thus yield an accurate estimate of the ionic selectivity of the paracellular path.

### Introduction

Epithelial cells are held together by junctional complexes encircling each cell (12). In a number of epithelia, these junctions offer little resistance to ion movement. Proximal convoluted tubules of *Necturus* (4,28) dog (8), rat (16), rabbit (22), *Ambystoma* (25) and *Triturus* (19) kidney as well as *Necturus* gallbladder (14), and rabbit ileum (22) are characterized by epithelial cells and conspicuous lateral intercellular spaces, joined at their apical surface by a junctional complex. This junctional complex which includes the Zonula Occludens together with the lateral intercellular spaces comprise the extracellular shunt path or paracellular pathway for transepithelial ion movement. Permeability and resistance properties of the two cell membranes in series as well as that of the shunt must be elucidated for the complete

characterization of transepithelial ion movement. Transepithelial ion movement has been studied in terms of the contributions made by the two cell membranes in series as well as the extracellular or paracellular shunt pathway in the *Necturus* proximal tubule (2,3,5,6,7). This work attempts to further clarify the role played by the paracellular shunt in passive ion movement. In the presence of transepithelial ion concentration gradients, the proximal tubular epithelium develops diffusion potentials which superimpose on the normal transepithelial potential difference. Using salt dilutions on either side of the epithelium and treating the resulting changes in transepithelial potential difference as a liquid junction potential, the relative transepithelial ion selectivity of the epithelium was assessed for sodium and chloride ions. Moreover determinations of potential differences and resistances during salt dilution were used to analyze the various elements of an equivalent electrical circuit of the proximal epithelium (2,5). Actual changes in the electromotive forces were computed both for the two cell membranes in series, luminal and peritubular, and for the paracellular pathway. These changes in equivalent electromotive forces were correlated with observed changes in potential difference across the same barriers. The results lend support to the view that the properties of the overall epithelium are characterized entirely by the paracellular pathway and that observed changes in transepithelial potential yield an accurate estimate of the ionic selectivity pattern of the shunt.

## Methods

### Animal Preparation

All experiments were performed on adult *Necturus maculosus* of either sex (Mogul-Ed, Oshkosh, Wisconsin). Doubly perfused kidneys of *Necturus* were prepared as previously described (17). The composition of control solutions, i.e., both superfusion fluid bathing the kidney surface and vascular perfusion fluid, was similar to the Ringer solution used previously, (2). Experimental superfusion and vascular perfusion solutions had the same ionic composition as Ringer solution except that a moiety of NaCl was replaced in isosmotic proportions by sucrose.

### Electrical Measurements

Peritubular ( $V_1$ ) or transepithelial ( $V_3$ ) electrical potential differences were recorded differentially, i.e., between an intracellular or intraluminal microelectrode and an external reference microelectrode by means of high impedance electrometers. Intracellular or intraluminal microelectrodes were of the Ling-Gerard type. Only microelectrodes with tip potentials less than  $\pm 5$ mV were used. The differential output of the electrometers was displayed on a Tektronix 502A dual-beam oscilloscope and recorded by means of a Gould Brush 220 recorder (Gould Inc, Cleveland, Ohio). All electrical potential measurements were made on early and mid-proximal convoluted surface tubules.

The following technique was employed in the measurement of dilution potentials during salt gradient experiments. A double-barrelled pipette for microperfusion was initially made to impale the lumen such that solutions could be rapidly switched on the luminal side of the cells. Transepithelial potential

differences,  $V_3$  as well as changes in this potential difference,  $\Delta V_3$  were monitored during unilateral salt dilutions in the lumen,  $l$ , or in the peritubular capillaries,  $p$ , and lumen simultaneously,  $pl$ . Four switches in solution were made in succession while the microelectrode impaled the lumen, according to the following protocol. The sequence of substitutions for tenfold dilutions was

$$\frac{(\text{NaCl})^p}{(\text{NaCl})^l} = \frac{100}{100} \rightarrow \frac{100}{10} \rightarrow \frac{10}{10} \rightarrow \frac{10}{100} \rightarrow \frac{100}{100}$$

$$\frac{(\text{NaCl})^p}{(\text{NaCl})^l}$$

where  $(\text{NaCl})$  represents the ratio of the sodium chloride concentration in the peritubular capillaries to that in the lumen. First, the peritubular capillaries and lumen were perfused with control Ringer solution  $c$ , and the transepithelial potential difference,  $V_3^c$  was recorded. Second, the luminal fluid was diluted by a factor of 10, an  $l$  substitution, and the transepithelial potential was recorded,  $V_3^l$ .  $\Delta V_3^l$  was calculated as  $V_3^l - V_3^c$ . Third, a bilateral substitution was made and the transepithelial potential,  $V_3^{pl}$  was recorded when both peritubular and luminal compartments,  $pl$ , were diluted by a factor of 10.  $\Delta V_3^{pl}$  was computed as  $V_3^{pl} - V_3^c$ , was obtained when the luminal fluid was returned to the control solution and the peritubular compartment remained diluted, a  $p$  substitution.  $\Delta V_3^p$  was taken as  $V_3^p - V_3^c$ . Finally, both compartments were returned to the control solution and  $V_3^c$  was again recorded. All substitutions occurred during a single impalement. Thus, the sequence of substitutions can be summarized as  $c, l, pl, p, c$  where  $c, l, pl, p$  are used as superscripts to indicate the conditions in which the absolute potential difference,  $V$ , and the change in potential difference from control,  $\Delta V$ , were obtained. The same procedure was followed for the twofold and fivefold sodium chloride dilutions. A switch from one perfusion solution to the next was made only after a steady state transepithelial potential difference was achieved. Reversing the sequence did not alter the results.

The measurements of peritubular membrane potential,  $V_1$  as well as changes in this potential,  $\Delta V_1$  were achieved during salt dilution experiments using the same protocol as above except that the recording microelectrode impaled the cell.

The ratio of luminal ( $R_2$ ) to peritubular ( $R_1$ ) cell membrane resistance, was evaluated from a direct measurement of the voltage divider ratio. Hyperpolarizing square wave currents from a constant current source were applied across a microelectrode within the tubular lumen. A second microelectrode in close proximity to the first, impaled a cell of the same tubule. As current was injected through the intraluminal microelectrode, a deflection of the peritubular membrane potential  $\Delta V_1$  was sensed by the intracellular microelectrode. The latter electrode was then advanced into the lumen at the same site. Again, upon current passage through the first microelectrode, a deflection of the transepithelial potential,  $\Delta V_3$  was detected by the second microelectrode. Deflections across the luminal cell membrane potential,  $\Delta V_2$ , were then calculated from the difference between  $\Delta V_3$  and  $\Delta V_1$ . The voltage divider ratio,  $\Delta V_2/\Delta V_1$  is a measure of  $R_2/R_1$ .

The specific resistance of early proximal tubules was measured by means of cable analysis experiments using the technique described earlier (4,8,18) and was determined from the measured length constant, the known resistivity of Ringer solution in the lumen, and the internal radius of the tubule (4).

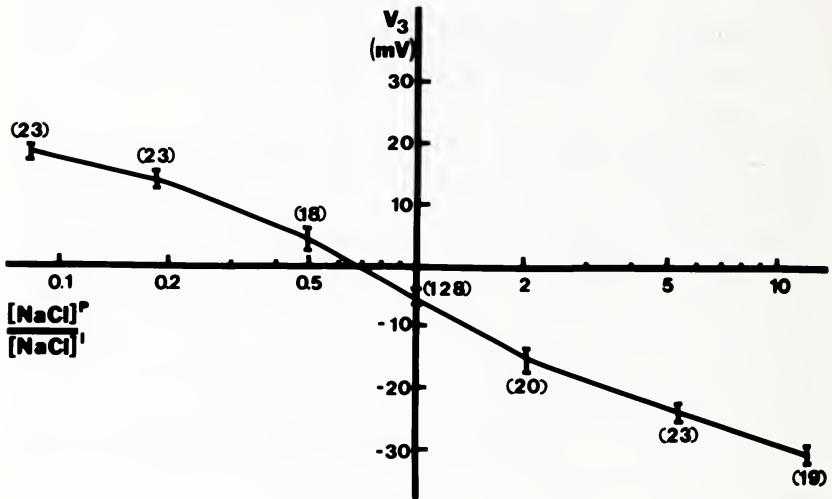


FIGURE 1. Magnitude of the transepithelial potential,  $V_3$ , during salt gradient experiments plotted against the logarithm of the sodium chloride concentration gradient. Mean values with  $\pm 1$  SE are shown. Number of observations are in parentheses.

## Results

### Salt dilution potential measurements

Figure 1 illustrates the results obtained for  $V_3$  during the imposition of three different sodium chloride concentration gradients. Measurements of  $V_3$  in mV are plotted on the ordinate and sodium chloride concentrations ratios,  $(NaCl)^p/(NaCl)^l$  are plotted on the abscissa. Luminal dilutions are shown on the right and peritubular dilutions are shown on the left. As can be seen from the graph, dilution of the intraluminal fluid, i.e. an  $l$  substitution, results in a hyperpolarization of the transepithelial potential. This is the case for all three dilution factors. On the other hand, dilution of the vascular compartment, i.e., a  $p$  substitution, results in a reversal of the transepithelial potential for all gradients studied. For both unilateral dilutions, the diluted compartment becomes more negative which implies preferential anionic selectivity of the tubular epithelium. In contrast, in superficial mammalian proximal convoluted tubule of rat and dog *in vivo*, (8,9,16), in isolated juxtamedullary proximal convoluted tubules (20), juxtamedullary proximal straight tubules (20,21) and in the first millimeter of isolated superficial proximal convoluted tubules (20) of rabbit kidney, it has been shown that the epithelium is cation selective. However, the second millimeter of isolated superficial proximal convoluted tubules (20) and the pars recta of superficial proximal tubules (21,26) of the rabbit exhibit a selectivity quite similar to the present findings.

Figure 1 also shows that salt gradients of equal magnitude but of reversed direction yield identical  $V_3$ 's but of opposite sign. The symmetry in response in absolute values for  $V_3$  implies that either the epithelium as a whole acts as a single barrier or that the two cell membranes in series, i.e., both the luminal and peritubular cell membranes, exhibit identical ion selectivity. This latter possibility is highly unlikely in view of previous findings (5,6,7) which show discrepant selectivity properties of the peritubular and luminal membrane particularly with respect to sodium ion permeability.

A quantitative estimate of the transference numbers for sodium ( $t_{Na}$ ) and chloride ( $t_{Cl}$ ) can be obtained if  $\Delta V_3$  is treated as a liquid junction potential. The change in transepithelial potential, the change in the sodium chloride concentration ratio in the two compartments, i.e., peritubular and luminal, and the transference numbers are related by the following equation:

$$\frac{dV^3}{d(\log \frac{[NaCl]_p}{[NaCl]_l})} = 2.3 \frac{RT}{F} (t_{Na} - t_{Cl})$$

where R is the universal gas constant, F is the Faraday constant, and T is the absolute temperature.

Figure 1 exhibits a non-linear behavior of  $V_3$  plotted against  $\log [NaCl]_p/[NaCl]_l$ . Therefore separate slopes were evaluated. For each dilution factor, data from  $V_3^c$ ,  $V_3^p$ ,  $V_3^l$ , and  $V_3^s$  were pooled to compute regression lines. Table 1 compares the calculated transference number  $t_{Cl}$  and  $t_{Na}$  together with the transference number ratio  $t_{Cl}/t_{Na}$  for different dilution factors. In all cases the transference number ratio exceeds the free solution chloride to sodium mobility ratio of 1.52.

Table 1  
Transference numbers for chloride and sodium

Dilution Factor	Average [NaCl]	$\frac{[NaCl]_p}{[NaCl]_l}$	$\frac{dV_3}{d(\log \frac{[NaCl]_p}{[NaCl]_l})}$	$t_{Cl}$	$t_{Na}$	$t_{Cl}/t_{Na}$
2	75 mM	0.5 & 2	-31.5 mV $\pm$ 3.4 (n=77)	0.77	0.23	3.36
5	60 mM	0.2 & 5	-25.4 mV $\pm$ 1.0 (n=92)	0.72	0.28	2.54
10	55 mM	0.1 & 10	-22.6 mV $\pm$ 0.6 (n=85)	0.69	0.31	2.27

Evidence presented thus far strongly suggests that the measured changes in transepithelial potential difference reflect the presence of a single barrier and are likely due to the selectivity of the paracellular pathway, rather than to two barriers, such as the two cell membranes, basolateral or peritubular membrane, and luminal membrane, in series.

Consider  $E_1$ ,  $E_2$ , and  $E_3$  as the equivalent ionic electromotive forces due to the diffusional pathways of respectively the peritubular cell membrane, the luminal cell membrane, and the paracellular shunt, and  $R_1$ ,  $R_2$ ,  $R_3$  the equivalent corresponding ionic resistances of these same barriers. The potential differences recorded across the peritubular cell membrane  $V_1$ , the luminal cell membrane

$V_2$ , and across the entire epithelium  $V_3$  are not simply related to the electrical parameters  $E$  and  $R$  of their own barrier but to the interplay of all three electromotive forces and all three ionic conductances combined (5). Equations relating these parameters have been reported earlier (2,5).

The presence of three boundaries across which diffusion potential differences may occur renders it impossible to study one barrier independently of the two others. Externally imposed changes in chemical potential as performed during salt dilutions always affect the chemical potential difference across two barriers simultaneously (5). For example, a peritubular salt dilution ( $p$ ) affects the diffusional pathways which are represented by  $E_1$  and  $E_3$ , a luminal salt dilution ( $l$ ) affects similarly  $E_2$  and  $E_3$ , whereas a symmetrical ion composition ( $pl$ ) would affect at least  $E_1$  and  $E_2$ .

In view of these problems of interpretation, additional information was gathered with the aim of at least resolving the true permeability characteristics of the paracellular pathway. For this purpose peritubular membrane potential differences,  $V_1$ , and changes in  $V_1$ ,  $\Delta V_1$  were also measured during salt dilutions of the same type as described above.

### Resistance measurements

The luminal to peritubular cell membrane resistance ratio, for the free flow condition in 19 proximal tubular impalements was  $2.82 \pm 0.25$  as shown in Table 2. This is not significantly different from a value of  $2.52 \pm 0.30$  ( $n=22$ ) obtained

Table 2

Experimental Potential Differences and Resistances

		$c$	$p$	$l$	$pl$
$V_1$	(mV)	$-52.89 \pm 1.50$ (19)	$-30.13 \pm 1.95$ (16)	$-42.06 \pm 1.56$ (17)	$-20.08 \pm 1.98$ (13)
$\Delta V_1$	(mV)		$+21.97 \pm 1.02$ (16)	$+10.76 \pm 0.80$ (17)	$+30.92 \pm 2.03$ (13)
$V_2$	(mV)	$+46.37$	$+48.84$	$+11.64$	$+13.58$
$\Delta V_2$	(mV)		$+1.70$	$-34.89$	$-31.60$
$V_3$	(mV)	$-6.52 \pm 0.81$ (28)	$+18.70 \pm 0.63$ (23)	$-30.42 \pm 1.43$ (19)	$-6.50 \pm 1.30$ (15)
$\Delta V_3$	(mV)		$+23.67 \pm 0.75$ (23)	$-24.13 \pm 0.99$ (19)	$-0.68 \pm 0.83$ (15)
$\frac{R_2}{R_1}$		$2.82 \pm 0.25$ (19)			
$R_{te}$	(ohm $cm^2$ )	$102.16 \pm 13.62$ (19)			

All values are means  $\pm$  SE

Numbers in parentheses refer to the number of observations.

$V_1$ ,  $V_2$ ,  $V_3$  are the mean peritubular, luminal, and transepithelial potentials.

$\Delta V_1$ ,  $\Delta V_2$ ,  $\Delta V_3$  are the changes in peritubular, luminal and transepithelial

potentials as compared to control during 1:10 salt dilution.

$R_2/R_1$  is the ratio of the luminal to peritubular cell membrane resistances.

$R_{te}$  is the specific transepithelial resistance.

$c$  refers to the control condition,  $p$  to unilateral peritubular substitution,  $l$  to unilateral luminal substitution,  $pl$  to bilateral peritubular and luminal substitutions.

previously (7). The specific resistance of the proximal tubule was measured by means of cable analysis experiments. The specific resistivity,  $R_i$ , of the intraluminal fluid was taken to be 100 ohm  $\text{cm}^2$  (4). The tubule radius,  $r$ , measured for 19 impalements of different early proximal tubules averaged  $60.47 \pm 1.56 \times 10^{-4}$  cm. The tubular length constant,  $\lambda$ , for the same tubules averaged  $531.36 + 36.32 \times 10^{-4}$  cm. This can be compared with a value of  $492.00 \pm 33.48 \times 10^{-4}$  cm ( $n=14$ ) for the blood perfused kidney also measured from early segments of the proximal tubule (4). The tubule radius,  $r$ , and length constant was determined experimentally and the specific resistance ( $R_{te}$ ), for each tubule was then calculated by means of the equation

$$R_{te} = \frac{2R_i \lambda^2}{r} \quad (2)$$

The specific transepithelial resistance for 19 tubules averaged  $102.16 \pm 13.62$  ohm  $\text{cm}^2$  as shown in Table 2. Again, this can be compared with a value for the blood perfused kidney of  $69.87 \pm 8.47$  ( $n = 14$ ) ohm  $\text{cm}^2$  (4).

#### Analysis of single electromotive forces and resistances

The observed changes in cellular and transepithelial potential difference together with the relative and absolute resistance measurements given in Table 2 may be combined to obtain information on the actual changes in electromotive forces of either the peritubular, luminal or paracellular barrier. In accordance with the equivalent electrical circuit for a shunted epithelium (2,5) observed changes in potential at any barrier,  $\Delta V$ , relate to actual changes in electromotive force,  $\Delta E$ , and resistances  $R$ , according to the following set of equations (3) to (8).

$$\Delta V^p = \frac{\Delta E^p (R_2 + R_3) + R_1 (\Delta E_3^p - \Delta E_2^p)}{R_1 + R_2 + R_3} \quad (3)$$

$$\Delta V_1^l = \frac{\Delta E_1^l (R_2 + R_3) + R_1 (\Delta E_3^l - \Delta E_2^l)}{R_1 + R_2 + R_3} \quad (4)$$

$$\Delta V_1^{pl} = \frac{\Delta E^{pl} (R_2 + R_3) + R_1 (\Delta E_3^{pl} - \Delta E_2^{pl})}{R_1 + R_2 + R_3} \quad (5)$$

$$\Delta V_2^p = \frac{\Delta E_2^p (R_1 + R_3) + R_2 (\Delta E_3^p - \Delta E_1^p)}{R_1 + R_2 + R_3} \quad (6)$$

$$\Delta V^p = \frac{\Delta E_2^l (R_1 + R_3) + R_2 (\Delta E_3^l - \Delta E_1^l)}{R_1 + R_2 + R_3} \quad (7)$$

$$\Delta V_2^{pl} = \frac{\Delta E_2^{pl} (R_1 + R_3) + R_2 (\Delta E_3^{pl} - \Delta E_1^{pl})}{R_1 + R_2 + R_3} \quad (8)$$

These equations relate changes in potential with changes in electromotive force and membrane resistances and are derived from the general expressions for  $V_1$ ,  $V_2$  and  $V_3$  as a function of  $E$ 's and  $R$ 's (5). The equations (3) to (8) assume that the resistances  $R_1$ ,  $R_2$ , and  $R_3$  are unaltered by the substitutions. The first three equations (3) to (5) show peritubular membrane potential changes  $\Delta V_1$  obtained during unilateral dilutions on the luminal side,  $l$ , peritubular side,  $p$ , and for bilateral dilutions,  $pl$ . The next three questions (6) to (8) show luminal membrane potential changes  $\Delta V_2$  obtained under the same conditions. Similar equations for  $\Delta V_3$  are not included since these equations would constitute a dependent set. The luminal to peritubular membrane resistance ratio,  $a$ , and the specific resistance of the epithelium,  $R_{te}$ , are also shown and explicitly stated in terms of the individual resistances in equations (9) and (10).

$$a = \frac{R_2}{R_1} \quad (9)$$

$$R_{te} = \frac{(R_1 + R_2) R_3}{R_1 + R_2 + R_3} \quad (10)$$

Equations (3), (4), (5), (6), (7), (8), (9), (10) constitute eight equations in twelve unknowns, i.e.,  $R_1$ ,  $R_2$ ,  $R_3$ ,  $E_1^p$ ,  $E_1^l$ ,  $E_1^{pl}$ ,  $E_2^p$ ,  $E_2^l$ ,  $E_2^{pl}$ ,  $E_3^p$ ,  $E_3^l$ ,  $E_3^{pl}$ . Six additional assumptions further reduce the number of unknowns. The assumptions are: (a)  $\Delta E_1^l = \Delta E_2^l = \Delta E_3^l = 0$ ; (b)  $\Delta E_1^p = \Delta E_2^p$ ; (c)  $\Delta E_2^l = \Delta E_3^l$  and (d)  $\Delta E_3^p = -\Delta E_3^l$ .

The first two equalities in (a) state that the cell membrane e.m.f. (luminal or peritubular) does not change during a change in chemical potential at the contralateral barrier (peritubular or luminal) respectively. The third equality states that changes in paracellular e.m.f. remain unaffected by bilateral substitutions. This implies the presence of a single membrane or symmetrical barrier. The latter assumption is justified by the demonstration of symmetrical responses of  $\Delta V_3$  during salt gradients of opposite sign. The assumptions in (b) and (c) state that the e.m.f. of a membrane will undergo the same independent change whether that membrane alone or also the contralateral membrane is exposed to an external concentration change. This holds for both the peritubular membrane and luminal membrane. The last assumption in (d) states that changes in shunt e.m.f. for luminal substitutions are equal but opposite in sign to shunt e.m.f. changes for peritubular substitutions. Again, this implies the presence of a symmetrical barrier. With these assumptions, the system is reduced to six independent equations, (11), (12), (13), (14), (5), (8), in six unknowns  $\Delta E_1^p$ ,  $\Delta E_2^p$ ,  $\Delta E_3^p$ ,  $R_1$ ,  $R_2$ ,  $R_3$  which can then be solved.

$$\Delta V_1^p = \frac{\Delta E_1^p (R_2 + R_3) + \Delta E_3^p R_1}{R_1 + R_2 + R_3} \quad (11)$$

$$\Delta V_1^l = \frac{-R_1 (\Delta E_2^l + \Delta E_3^l)}{R_1 + R_2 + R_3} \quad (12)$$

$$\Delta V_2^p = \frac{R_2 (\Delta E_3^p - \Delta E_1^p)}{R_1 + R_2 + R_3} \quad (13)$$

$$\Delta V_2^l = \frac{\Delta E_2^l (R_1 + R_3) - \Delta E_3^l R_2}{R_1 + R_2 + R_3} \quad (14)$$

Using this set of equations, the various single barrier  $\Delta E$ 's and  $R$ 's were calculated and are listed in the left column of Table 3. Observed  $\Delta V$  values for  $p$ ,  $l$ , and  $pl$  substitutions are shown for comparison in the right column. All  $\Delta V_2$  values have been calculated from measured  $\Delta V_3$  and  $\Delta V_1$  values for all substitutions. As can be seen, the  $\Delta E_1$ 's and  $\Delta V_1$ 's approximate one another for peritubular salt dilutions only. No correlation exists between  $\Delta E_2$  and  $\Delta V_2$  for any of the substitutions, whereas there is a complete agreement between  $\Delta E_3$  and  $\Delta V_3$  in all conditions.

In addition, solution of the equations also yields quantitative information concerning cell membrane resistances. The luminal membrane,  $R_2$  is found to have almost free times the resistance of the peritubular membrane,  $R_1$ , with absolute values shown in Table 3. Paracellular resistance,  $R_3$ , is calculated to be 103 ohm  $\text{cm}^2$ , very close to the overall measured transepithelial specific resistance of 102 ohm  $\text{cm}^2$ . Calculated values for  $R_1$  and  $R_2$  are moreover close to the resistance values obtained experimentally by means of cable analysis for proximal tubules of *Necturus* (1,28) and *Triturus* (19).

Table 3

Calculated parameters	Observed potential changes
$\Delta E_1^l = +21.37$ mV	$\Delta V_1^l = +21.97$ mV
$\Delta E_1^l = 0$ mV	$\Delta V_1^l = +10.76$ mV
$\Delta E_1^{pl} = +21.37$ mV	$\Delta V_1^{pl} = +30.92$ mV
$\Delta E_2^l = 0$ mV	$\Delta V_2^l = +1.70$ mV
$\Delta E_2^l = +65.23$ mV	$\Delta V_2^l = -34.89$ mV
$\Delta E_2^{pl} = -65.23$ mV	$\Delta V_2^{pl} = -31.60$ mV
$\Delta E_3^l = +23.69$ mV	$\Delta V_3^l = +23.67$ mV
$\Delta E_3^l = -23.69$ mV	$\Delta V_3^l = -24.13$ mV
$\Delta E_3^{pl} = 0$ mV	$\Delta V_3^{pl} = -0.68$ mV
$R_1 = 2,550$ ohm. $\text{cm}^2$	
$R_2 = 7,192$ ohm. $\text{cm}^2$	
$R_3 = 103$ ohm. $\text{cm}^2$	

$\Delta E_1$ ,  $\Delta E_2$ ,  $\Delta E_3$  are the calculated changes in e.m.f. induced by a tenfold salt dilution across the peritubular, luminal, and paracellular barriers.

### Discussion

The present electrical measurements provide firm evidence for the important role an extracellular or paracellular shunt path plays in the overall transepithelial conductance of the proximal tubules of *Necturus* kidney.

Relative chloride to sodium transference numbers obtained indicate that the paracellular path behaves as an anion-selective barrier. The great majority of leaky epithelia exhibit an opposite cation selective permeability pattern where sodium permeability dominates chloride permeability. Such is the case for proximal convoluted tubules of the *in vivo* rat kidney (9,16) and autoperfused dog kidney (8), the juxtamedullary convoluted segments (20) of isolated rabbit proximal tubule, fish gallbladder (11), rabbit gallbladder (11, 13), bullfrog gallbladder (23), mammalian small intestine (13,29) and tortoise small intestine (30).

Preferential anion permeation in the amphibian proximal tubule may result from the epithelium acting as an anion-exchange membrane with fixed or mobile sites (27). Alternatively the sites within the pores or channels controlling transepithelial ion movement may be electroneutral with polar pores such that the positive charge of the dipole protrudes into the center of the pore, thus facilitating anion transfer.

Transepithelial potential differences yield a non-linear but symmetrical response to the imposition of salt gradients across the epithelium. The preferential permeability for chloride or the  $t_{Cl}/t_{Na}$  ratio decreased with either increased absolute gradient, larger dilution factor or with decreased average salt concentration in the permeation barrier. Similar relationships between transepithelial potential difference and sodium chloride concentrations of salt gradients have been reported in rat proximal tubule (15).

Relationships between transepithelial potential and salt concentration also deviate from linearity in rabbit ileum (13). Asymmetrical responses elicited by composition changes of solutions on opposing sides of leaky epithelia have occasionally been reported but are probably due to the presence of different unstirred layers on either side (29,30). Linear and symmetrical responses of transepithelial potential difference to unilateral salt gradients of opposite polarity but equal magnitude have been found in fish gallbladder (10), rabbit gallbladder (11) and bullfrog gallbladder (23).

The kind of deviation in the behavior of the selectivity shown in Figure 1 and Table 1 indicates a dependence of the relative chloride to sodium permeability on either the absolute value of the concentration difference or on the average concentration of the salt in the diffusion barrier. It is interesting to note that a  $t_{Cl}/t_{Na}$  ratio close to the free solution mobility ratio was found in a 1:20 dilution (7).

The present study provides direct evidence that the observed transepithelial potential changes originate from a single permselective path i.e., the paracellular shunt. The symmetry of the transepithelial voltage-salt concentration plots suggest the presence of a single barrier, and a selectivity due to the extracellular shunt rather than to the two cell membranes in series. In order to firmly establish this point, changes in transepithelial potential differences and changes in cell

membrane potential difference were correlated with the actual changes in electromotive forces generated across these same barriers. The results of this analysis clearly confirm the view that the changes in both the luminal and peritubular cell membrane potential differences cannot be completely accounted for in terms of actual changes in the electromotive forces generated across these same barriers (2,3,5). On the contrary, as predicted, the changes in transepithelial potential differences can be completely accounted for in terms of changes in electromotive force generated across the shunt. The observed selectivity pattern of the entire epithelium as calculated from  $\Delta V_3$  describes accurately the relative contribution of chloride and sodium to the diffusional pathways along the paracellular route.

Finally, it is important to note that the entire analysis employed in the present study has considered only dissipative processes at each of the membrane barriers. Inclusion of active transport pumps behaving as constant current sources greatly complicates the interpretation of electrical potential differences induced by changes in external chemical potential (5).

In conclusion, the data support the view of the existence of a low paracellular shunt resistance and electrical coupling between contralateral cell membranes in the proximal tubule of the Necturus. The properties of the overall epithelium seem to be almost entirely determined by the paracellular pathway. This path is governed by a simple symmetrical membrane, perhaps electrically neutral or of a certain fixed charge density. In contrast to the mammalian kidney and other leaky epithelia, the proximal tubular wall of the Necturus kidney is anion selective. Transepithelial potential changes observed are close estimates of the actual changes in the paracellular electromotive force. Hence, imposed transepithelial diffusion potentials across this "leaky" epithelium measure accurately the ionic selectivity of the paracellular shunt pathway.

### Acknowledgements

The authors wish to thank the Connecticut Heart Association and the National Institute of Health for funding this research.

### Literature Cited

1. ANAGNOSTOPOULOS, T. and E. VELU. 1974. Electrical resistance of cell membranes in Necturus kidney. *Flugers Arch.* 346:327-399.
2. BOULPAEP, E. . 1967. Ion permeability of the peritubular and luminal membrane of the renal tubular cell. In "Transport and Funktion intracellulärer Elektrolyte", edit F. Kruck, Urban and Schwarzenberg, 98-107.
3. BOULPAEP, E. L. 1971. Electrophysiological properties of the proximal tubule: Importance of cellular and intercellular transport pathways. In: *Electrophysiology of Epithelial Cells*, Stuttgart, F. K. Schattauer Verlag, 91-118.
4. BOULPAEP, E. L. 1972. Permeability changes of the proximal tubule of Necturus during saline loading. *Am. J. Physiol.* 222:517-531.
5. BOULPAEP, E. L. 1976. Electrical phenomena in the nephron. *Kidney Int.* 9:88-102.
6. BOULPAEP, E. L. Electrophysiology of the proximal tubule of Necturus kidney. I. The peritubular cell membrane. *J. Gen. Physiol.* submitted.

7. BOULPAEP, E. L. Electrophysiology of the proximal tubule of *Necturus* kidney. II. The luminal cell membrane and the paracellular pathway. *J. Gen. Physiol.* submitted.
8. BOULPAEP, E. L. and J. F. SEELY. 1971. Electrophysiology of proximal and distal tubules in the autoperfused dog kidney. *Am. J. Physiol.* **221**:1084-1096.
9. DE MELLO G. B., A. G. LOPES and G. MALNIC. 1976. Conductances, diffusion and streaming potentials in the rat proximal tubule. *J. Physiol. (London)* **260**:553-569.
10. DIAMOND, J. M. 1962. The mechanism of solute transport by the gallbladder. *J. Physiol. (London)* **161**:474-502.
11. DIAMOND, J. M. and S. C. HARRISON. 1966. The effect of membrane fixed charges on diffusion potentials and streaming potentials. *J. Physiol.* **183**:37-57.
12. FARQUHAR, M. G. and G. E. PALADE. 1963. Junctional complexes in various epithelia. *J. Cell Biol.* **17**:375-412.
13. FRIZZELL, R. a. and S. G. SCHULTZ. 1972. Ionic conductances of extracellular shunt pathway in rabbit ileum. Influence of shunt on transmural sodium transport and electrical potential differences. *J. Gen. Physiol.* **59**:318-346.
14. FROMTER, E. 1972. The route of passive ion movement through the epithelium of *Necturus* gallbladder. *J. Membrane Biol.* **8**:259-301.
15. FROMTER, E., C. W. MULLER and H. KNAUF. 1968. Fixe neative Wandladungen im proximalen Konvolut der Rattenniere and inre Beeinflussung durch Calciumionen. 6th Symp. Gesellschaft Nephrol., Vienna, p. 61-64.
16. FROMTER, E., C. W. MULLER and T. WICK. 1971. Permeability properties of the proximal tubular epithelium of the rat kidney studied with electrophysiological methods. In "Electrophysiology of Epithelial Cells, Stuttgart, F. K. Schattauer Verlag, p. 119-148.
17. GIEBISCH, G. 1961. Measurement of electrical potential difference on single nephrons of the perfused *Necturus* kidney. *J. Gen. Physiol.* **44**:659-678.
18. GRANDCHAMP, A., and E. L. BOULPAEP. 1974. Pressure control of sodium reabsorption and intercellular backflux across proximal kidney tubule. *J. Clin. Invest.* **54**:69-82.
19. HOSHI. T. and F. SAKAI. 1967. A comparison of the electrical resistances of the surface cell membrane and cellular wall in the proximal tubule of the newt kidney. *Jap. J. Physiol.* **17**:627-637.
20. JACOBSON, H. R. and J. P. KOKKO. 1976. Intrinsic differences in various segments of the proximal convoluted tubule. *J. Clin. Invest.* **57**:818-825.
21. KAWARMURA, S., M. IMAI, D. W. SELDIN and J. P. KOKKO. 1975. Characteristics of salt and water transport in superficial and juxtamedullary straight segments of proximal tubules. *J. Clin. Invest.* **55**:1269-1277.
22. LUTZ, M. D., J. CARDINAL, and M. B. Burg. 1973. Electrical resistance of renal proximal tubule perfused in vitro. *Am. J. Physiol.* **225**:729-734.
23. MORENO, J. H. and J. M. DIAMOND. 1975. Cation permeation mechanism and cation selectivity in tight junctions of gallbladder epithelium. In "Membranes—A series of advances", Vol. 3, lipid bilayers and biological membranes: dynamic properties, p. 383-497.
24. ROSE, R. C. and S. G. SCHULTZ. 1971. Studies on the electrical potential profile across rabbit ileum. Effects of sugars and amino acids on transmural and transmucosal electrical potential differences. *J. Gen. Physiol.* **57**:639-663.
25. SACKIN, H., and E. L. BOULPAEP. 1976. Simultaneous intracellular and transepithelial potential measurements in isolated perfused amphibian proximal tubules. *Kidney Int.* **10**:597.
26. SCHAFER, J. A., S. L. TROUTMAN and T. E. ANDREOLI. 1974. Volume reabsorption, transepithelial potential differences, and ionic permeability properites in mammalian superficial proximal straight tubules. *J. Gen. Physiol.* **64**:582-607.
27. TEORELL, T. 1953. Transport process and electrical phenomena in ionic membranes. *Progr. Biophys. Biophys. Chem.* **3**:305-369.
28. WINDHAGER E. E., E. L. BOULPAEP and G. GIEBISCH. 1967. Electrophysiological studies on single nephrons. *Proc. Intern. Congr. Nephron., 3rd, Washington 1966, Basel, Karger, Vol. I, p. 35-47.*

29. WRIGHT, E. M. 1966. Diffusion potentials across the small intestine. *Nature*, 212:189-190.
31. WRIGHT, E. M., P.H. Barry and J. M. DIAMOND. 1971. The mechanism of cation permeation in rabbit gallbladder. Conductances, the current voltage relation, the concentration dependence of anioncation discrimination, and the calcium competition effect. *J. Membrane Biol.* 4:331-357.

